HITTITE JOURNAL OF SCIENCE AND ENGINEERING

e-ISSN: 2148-4171
Volume: 12 • Number: 3
September 2025

Fabrication of Functionally Graded Porous Materials via Additive Manufacturing and Investigation of Compressive Behavior

Ziya Burak Karaboğa | **Nihal Yumak***
Afyon Kocatepe University, Department of Mechanical Engineering, Gazlıgöl Road, 03200 Afyonkarahisar, Türkiye.

Corresponding Author
Nihal Yumak
E-mail: nyumak@aku.edu.tr Phone: +90 553 972 6800
RORID: https://ror.org/ror.org/03a1crh56

Article Information
Article Type: Research Article
Doi: https://doi.org/10.17350/HJSE19030000360
Received: 07.05.2025
Accepted: 03.08.2025
Published: 30.09.2025

Cite As
Karaboğa ZB, Yumak N. Fabrication of Functionally Graded Porous Materials via Additive Manufacturing and Investigation of Compressive Behavior. Hittite J Sci Eng. 2025;12(3):137-143.

Peer Review: Evaluated by independent reviewers working in at least two different institutions appointed by the field editor.
Ethical Statement: Not available.
Plagiarism Checks: Yes - iThenticate
Conflict of Interest: There is no conflict of interest between the authors.

CRediT AUTHOR STATEMENT
Ziya Burak KARABOĞA: Design and fabrication of test specimens, execution of mechanical tests, data analysis
Nihal YUMAK: Design and fabrication of test specimens, review & editing, overall supervision and guidance.

Fabrication of Functionally Graded Porous Materials via Additive Manufacturing and Investigation of Compressive Behavior

Ziya Burak Karaboğa | Nihal Yumak*

Afyon Kocatepe University, Department of Mechanical Engineering, Gazlıgöl Road, 03200 Afyonkarahisar, Türkiye.

Abstract

In this study, functionally graded (FG) porous materials containing one or more infill patterns and infill rates were designed to fabricate porous materials with high compressive properties. For the FG material design, five types of infill patterns (three 3D infill patterns: octet, gyroid, and cubic; and two 2D infill patterns: trihexagonal and concentric) and two infill rates (50% and 70%) were determined. Utilizing various combinations of different infill rates and infill patterns, a total of 21 FG porous samples and 5 control samples with uniform porous distribution were designed. The samples were produced using the Fused Deposition Modelling (FDM), and the effect of functional grading on the compressive behavior of the porous material was investigated by conducting compression tests using an Instron 8801 testing machine. The highest compressive strength was obtained in the 70%CONS sample, which was functionally graded based on infill rate, with a 54% increase compared to its corresponding control sample. By combining the concentric 2D infill pattern with the gyroid 3D infill pattern, the compressive strength of the designed GY-CONS-GY sample increased by 33% compared to the gyroid sample.

Keywords: Functionally graded porous materials, additive manufacturing, fused deposition modelling, infill pattern, infill rate, compressive strength, PLA

INTRODUCTION

Nowadays, known as additive manufacturing (AM), the production method first emerged as a rapid prototyping method in 1988 [1]. In the next 30 years, it evolved into a preferred production method in many fields like biomedical, aerospace, defense, construction and automotive industry [2]. AM can be defined as a new-generation manufacturing technique designed to produce complex geometries by adding material layer by layer using 3D model data [3]. The leading advantages of AM compared to traditional production methods are design flexibility, the ability to produce complex geometries with high accuracy and low cost, low material waste, and no need for molds and similar tools in mass production [4]. In addition to all these advantages, advancements in AM technologies have expanded the range of producible materials, enabling the easy production of metals, ceramics, composites, and polymers [5].

Fused deposition modeling (FDM) is an additive manufacturing method that enables the production of 3D parts by melting thermoplastic filament material and extruding it from a nozzle [4]. The FDM method has become a highly preferred AM method due to its many advantages such as not requiring chemical or thermal post-processing after production, low cost of printers, low spare parts and maintenance costs compared to other devices, affordable filaments, and allowing the determination of mechanical properties of parts with process parameters [5]. Literature research has shown that process parameters such as infill angle, layer thickness, infill rate, infill pattern, build orientation, printing speed, number of wall layers, material type, nozzle and table temperature affect the mechanical properties of parts produced with the FDM method[4], [6]. Marşavina et al. investigated the effect of the process parameters such as building direction, 3D-printer type, building orientation, layer thickness, specimen thickness, and filament color on the tensile and fracture properties [7]. The study showed that there is a strong correlation between mechanical properties and process parameters. Infill patterns are divided into two groups based on their unit cell geometry. 2D infill patterns such as Grid, Lines, Triangle, Concentric, Zigzag, Cross and Trihexagonal maintain a consistent geometry across layers and primarily carry loads along the build direction[8]. However, 3D infills patterns such as Cubic, Gyroid, Octet, Tetrahedral, Cross 3D and Quarter Cubic have the capacity to distribute the load multi direction more evenly because of volumetric unit cell. Nevertheless, these patterns might decrease strength and stiffness in the building direction compared to the 2D patterns. In their study, Ivorra-Martinez et al. investigated the relationship between the infill rate and pattern by producing tensile and Charpy impact test specimens using FDM, employing infill rates of 20%, 60%, and 90%, along with 2D infill patterns such as rectilinear, honeycomb, and the Hilbert curve[9]. It was observed that the difference between the infill patterns was more pronounced at low infill rates, and the difference between the patterns decreased with increasing infill rates. In another study, bending test specimens with different infill rates (25%, 50% and 70%) and infill patterns (2D grid and honeycomb, 3D gyroid) were produced [10]. The results showed that the strength increased with the increase in infill rate as expected and the gyroid and honeycomb patterns showed higher strength than the grid infill patterns. In another study, compression test specimens were produced with 6 different 2D infill patterns (Hilbert curve, honeycomb, line, rectilinear, Archimedean curve and octagram spiral) at infill rate varying between 20-80% [11]. The results showed that the highest compressive strength was obtained as 121.35 MPa in the Hilbert curve, while the lowest compressive strength was obtained as 60.01 MPa in the octagram spiral. In all these studies, it was observed that both the infill pattern and the infill rate did not change throughout the sample and had a uniform distribution. However, in biomedical applications and the aerospace industry where additive manufacturing methods are frequently utilized it is important to understand not only the individual effects of process parameters such as infill pattern and infill rate, but also the interactions between them. In a study conducted on this subject, in order to design bone fixation plates that are more compatible with the human bone structure, the infill pattern and infill rate along the plate were functionally graded[12]. Thus, bone fixation plates with high porosity and high strength that allow osteointegration with low Elasticity modulus compatible with human bone structure could be produced. In a different study, Tanveer et

al. investigated the effect of infill rate on tensile and impact strength of functionally graded porous samples in their studies [13]. In the study, functionally graded porous samples were produced by dividing the cross-sectional area into three equal sections and assigning infill rates of 50%, 75%, and 100% to each part. The results showed that both tensile and impact behaviors changed significantly with the functional grading of the infill rate. Samples with a higher infill rate in the outer regions exhibited greater tensile strength, as cracks were observed to initiate from these areas. In another study, bamboo-inspired, honeycomb and cubic infill patterns were designed as functionally graded with varying strut diameters and the compression test results of the samples were compared with samples with homogeneous strut structure [14]. The results of the study showed that functional grading increased the compression modules, initial peak strength and energy absorption ability.

An analysis of the existing literature shows that process parameters such as infill rate and infill pattern play an important role in determining the mechanical properties of parts produced using the FDM. In addition, it has been determined that the porous structures obtained through functional grading of these process parameters have high application potential, especially in biomedical fields. A survey of the relevant studies reveals that it is striking that studies on functional grading are quite limited, and that the existing research predominantly focuses on similar and repetitive infill patterns and it has been observed that there is a need for a comprehensive systematic study in this field. For this reason, this study combines 3D (octet, gyroid and cubic) and 2D (trihexagonal and concentric) infill patterns, which is a relatively new topic in the literature, and designs functionally graded compression test specimens according to the infill pattern. In addition, another group of samples was functionally graded based on their infill rate and compression tests were applied to eliminate this deficiency in the literature.

MATERIAL AND METHODS

Design of Compression Test Samples

Compression test specimens were designed in two categories: functionally graded (FG) porous samples and uniformly porous control samples in accordance with ASTM D695 standard, as shown in Figure 1a[15]. In order to better observe the effect of functional grading, the samples were designed without enclosing walls on the side surfaces as well as the top and bottom faces. Control samples were produced using gyroid, trihexagonal, octet, concentric and cubic infill patterns, each with a 50% infill rate, as shown in Figure 1b. Compression test specimens were designed using ANSYS SpaceClaim and prepared for production via FDM using the Cura slicer software. The grading process was done according to the infill pattern and infill rate. Initially, the compression test samples were divided into three equal regions in the vertical direction using the Cura software, as illustrated in Figure 1c. In the samples graded according to infill rate, the middle part was produced with a 70% infill rate, and the upper and lower parts were produced with a 50% infill rate. The FG samples, according to the infill pattern, had the middle part produced with the 1st type of infill pattern, and the upper and lower parts produced with the 2nd type of pattern (Figure 1d). The infill rate in these samples was determined to be constant at 50% throughout the sample.

Table 1 The coding system used for control and FG porous samples

Sample Coding	Porous Geometry Pattern
Uniformly porous control samples	
GY	50% Gyroid
T	50% Trihexagonal
O	50% Octet
CONS	50% Concentric
C	50% Cubic
FG porous samples according to the infill rate	
70%GY	50% -70%-50% Gyroid
70%T	50% -70%-50% Trihexagonal
70%O	50% -70%-50% Octet
70%CONS	50% -70%-50% Concentric
70%C	50% -70%-50% Cubic
FG porous samples according to infill pattern	
GY-T-GY	50% Gyroid- 50% Trihexagonal - 50% Gyroid
GY-O-GY	50% Gyroid- 50% Octet- 50% Gyroid
GY-CONS-GY	50% Gyroid- 50% Concentric - 50% Gyroid
GY-C-GY	50% Gyroid- 50% Cubic - 50% Gyroid
T-GY-T	50% Trihexagonal- 50% Gyroid - 50% Trihexagonal
T-O-T	50% Trihexagonal- 50% Octet - 50% Trihexagonal
T-CONS-T	50% Trihexagonal- 50% Concentric - 50% Trihexagonal
T-C-T	50% Trihexagonal- 50% Cubic-50% Trihexagonal
O-GY-O	50% Octet- 50% Gyroid - 50% Octet
O-T-O	50% Octet- 50% Trihexagonal - 50% Octet
O-CONS-O	50% Octet- 50% Concentric - 50% Octet
O-C-O	50% Octet- 50% Cubic-50%Octet
C-GY-C	50% Cubic- 50% Gyroid - 50% Cubic
C-T-C	50% Cubic- 50% Trihexagonal - 50% Cubic
C-O-C	50% Cubic- 50% Octet - 50% Cubic
C-CONS-C	50% Cubic- 50% Concentric- 50% Cubic

All produced sample groups and the coding systems used for these samples are given in Table 1.

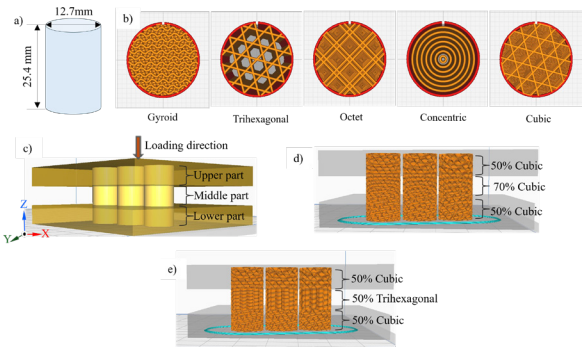

Figure 1 Design of compression test samples, a) Sample sizes in accordance with the ASTM D695 standard, b) Infill patterns, c) The division of the samples into three regions, d) FG samples based on the infill rate, e) FG samples according to the infill pattern.

Fabrication of Test Samples

The specimens were fabricated via the FDM with the Creality Ender 3 Pro 3D printer (Figure 2a). 1.75 mm thick PLA+ filament from the Microzey brand was used as the printing material. PLA+ filament is an improved material that provides higher durability, better layer adhesion and increased printing speed compared to standard PLA, while maintaining its low odor and environmentally friendly characteristic [16]. All control and FG porous compression test samples were weighed three times using a precision balance. The tensile properties of the filament material were determined through tensile tests conducted on samples fabricated with 100% infill in accordance with the ASTM D638 standard [17]. Tensile test was repeated three times using Instron 8801 tensile-compression test device with 2mm/min loading rate. Young's modulus, yield strength, and failure strain were found to be 2.93 GPa, 31 MPa, and 0.014 respectively. Printing parameters used during the manufacturing of compression and tensile test samples are listed in Table 2.

Table 2 Common printing parameters used for specimens.

Parameter	Value
Material	Polylactic Acid (PLA)
Printing rate	50 mm/s
Layer thickness	0.2 mm
Table temperature	60°C
Nozzle temperature	210°C
Wall thickness	0
Building orientation	On the X-Y plane, along Z axis

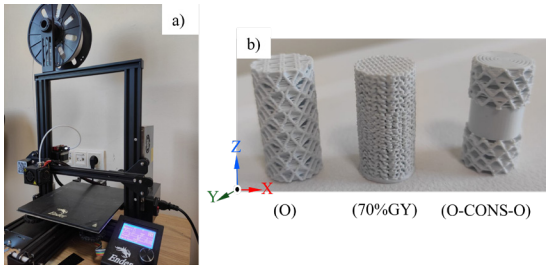

Figure 2 Fabrication of the test specimens, a) Creality Ender 3 Pro 3D printer, b) Compression test samples.

Compression Test Procedure

Compression tests were performed using the Instron 8801 tensile-compression test device. Samples were positioned between the jaws, and the test was conducted at a constant loading rate of 2 mm/min until the strain level reached 0.6. This strain value was determined in preliminary tests as the point at which all pores in the samples were fully collapsed. Compression tests were conducted three times for each specimen, and the average values were reported. Compression test stress-strain curves consist of inner regions as elastic, plateau and densification regions. Yield strength is found in elastic region with 0.2% offset methods and Young's modulus is found by calculating the slope of elastic region. Compression strength is calculated as the highest stress value measured in all regions. The energy absorbed (EA) during the compression test was determined by calculating the area under the stress-strain curve, as described in Equation 1 [18]. In the equation, ε represents the instantaneous strain, and σ represents the instantaneous stress. The energy absorbed per unit mass, known as the specific energy absorption (SEA), is calculated by dividing the EA by the mass (m) of the sample (Eq 2).

$$\mathrm{EA} = \int_0^{\varepsilon} \sigma(\varepsilon)\mathrm{d}\varepsilon \tag{1}$$

$$\mathrm{SEA} = \frac{\mathrm{EA}}{m} \tag{2}$$

The densification region was calculated using the maximum efficiency method (MEM) and the formula given in Equation 3[19]. The energy efficiency coefficient (η_e) is a coefficient obtained by dividing the area under the stress-strain curves by the instantaneous stress, and the point where it reaches its maximum value is the beginning of the densification zone.

$$\eta_e = \frac{1}{\sigma}\int_0^{\varepsilon} \sigma(\varepsilon)d\varepsilon, 0 < \varepsilon < 1 \tag{3}$$

RESULTS AND DISCUSSION

Compression Test Results of Control Samples

The stress-strain and strain-energy efficiency coefficient curves indicate that the compressive properties of the samples are strongly influenced by the infill patterns. As shown in Figure 3, 3D (GY, C and O) and 2D (CONS and C) control samples generally exhibit distinct characteristics across different regions of the stress–strain curve. Nevertheless, in the elastic region of stress-strain curve, all the control samples exhibited similar behavior, at this stage stress increased linearly with strain. However, beyond the elastic region, with the onset of plastic deformation stage stress-strain curve exhibited more stable characteristics in the GY, O, and C samples, whereas the T and CONS samples showed significant fluctuations in the stress levels. Because of their geometry, 3D infill patterns such as gyroid, octet and cubic distribute the load more evenly than concentric and trihexagonal 2D patterns[8]. After the plateau region, densification region was observed most rapidly in the CONS sample at a strain value of 0.38, while the latest densification

was observed in the T sample at a strain value of 0.53. This observation shows that the T sample can gradually absorb the energy over a longer deformation time, whereas in the CONS sample, the densification zone starts early due to the rapid collapse of the pores as a result of the localized transfer of the load due to the infill pattern. In the densification region, the pores completely collapsed, and the sample started to take solid form, and the voids originating from the unit pore geometry in the samples started to disappear. Therefore, the highest stress values were obtained in this region in all control samples except the T sample. The highest stress value in the T sample was encountered immediately after the elastic region. Among the control samples, the highest compressive stress level was recorded in the CONS sample as 40 MPa±4,2 in the densification stage.

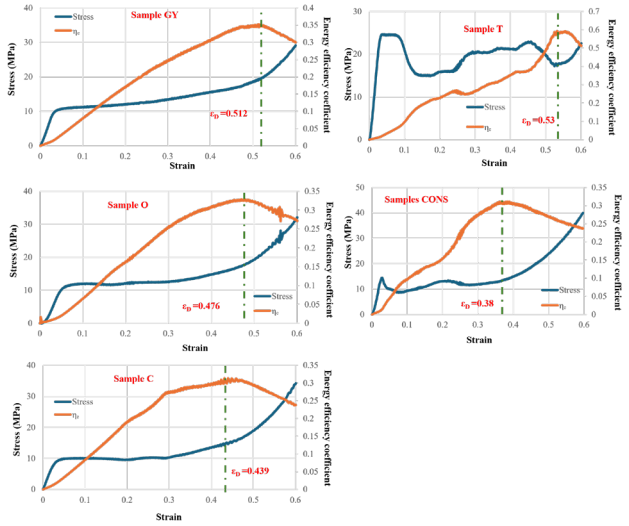

Figure 3 Compression test results of control samples.

Compression Test Results of FG Samples Based on Infill Rate

Functional grading according to the infill rate has led to a more gradual deformation mechanism as seen in Figure 4. Under compressive loading, the sections with 50% infill rate initially deformed and absorbed the applied energy, and the section with 70% infill rate in the middle section did not deform at first. As can be seen, this situation continued in this way until the 0.4 strain value. After the 0.4 strain value, as the load increased, the deformation progressed towards this high-density middle region and thus damage began to occur in the region with 70% infill rate. During the test, the progression of deformation occurred in a controlled and gradual manner depending on the density distribution of the material.

Figure 4 Deformation stages of 70%GY sample during compression loading.

The stress–strain curves of the FG samples based on the infill rate show similar behavior in the elastic region to the control samples with the same infill pattern (Figure 5). This characteristic of the curves can be explained by the fact that the deformation initially began in the regions with 50% infill rate at the bottom and top of the samples, and then, the deformation progressed into the region with 70% filling rate in the following stages. Therefore, the elastic region observed in the stress-strain curves and the corresponding values are very similar to those of the control samples (Figure 7). However, differences were observed in the plateau and densification regions of the stress-strain curve, with densification appearing to start at much earlier strain levels in the 70%T and 70%CONS samples with the 2D infill patterns, compared to their counterpart control samples. Nevertheless, in the 3D infill pattern (70%GY, 70%C and 70%O) the onset of densification stage was delayed to higher strain levels.

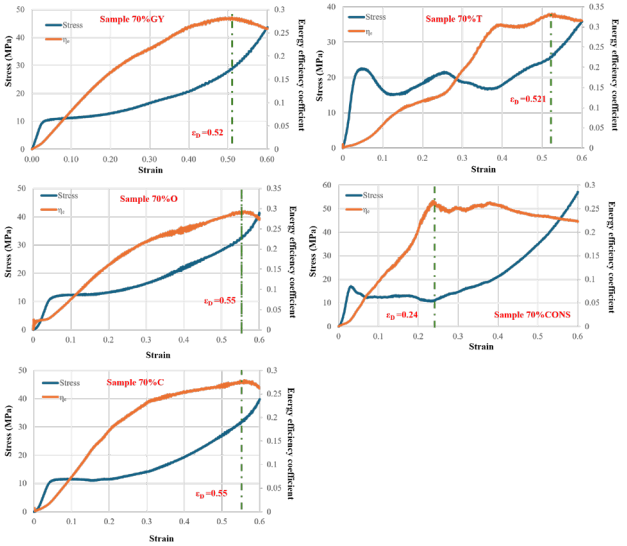

Figure 5 Compression test results of FG samples based on infill rate.

Compression Test Results of FG Samples Based on Infill Pattern

In Figure 6, stress-strain curves and strain-energy efficiency coefficient curves of functionally graded samples according to infill pattern are presented. Significant differences were obtained in elastic, plateau and densification regions of the samples containing both 3D and 2D infill patterns. Higher stress values were recorded in the elastic region of GY-T-GY and GY-CONS-GY samples' stress-strain curves compared to the GY control sample. On the other hand, stress values in the elastic region of GY-O-GY and GY-C-GY samples were found to be lower than those of control samples. This phenomenon can be explained by the fact that 2D patterns integrated into gyroid pattern provide higher yield strength by increasing stiffness of the sample. The stress values of the T-GY-T, T-O-T, and T-C-T samples recorded in the elastic region decreased significantly due to the addition of the 3D gyroid, octet and cubic infill pattern to the middle section of the samples. However, a similar situation was observed in the T-CONS-T sample, where two 2D pattern were together. In this sample, interfacial adhesion problems between the infill patterns caused the stress values in the elastic region to decrease. The

deformation manner of the T-GY-T, T-O-T and T-C-T samples was more stable compared to the T sample, thanks to the ability of the 3D infill patterns to distribute the load more uniformly and isotopically. However, the stress-strain curve in the plateau region of the T-CONS-T sample followed a wavy trend and deformation progressed irregularly due to the use of two 2D patterns together. The maximum stress value in the densification region of the GY-T-GY and GY-CONS-GY samples increased compared to the GY control sample, while this value decreased in GY-O-GY and GY-C-GY samples. A similar situation was observed in the functionally graded versions of the octet and cubic 3D patterns. These results suggest that 2D patterns integrated into the 3D infill pattern increase the compressive strength of the sample, whereas the addition of a second 3D pattern may reduce the strength.

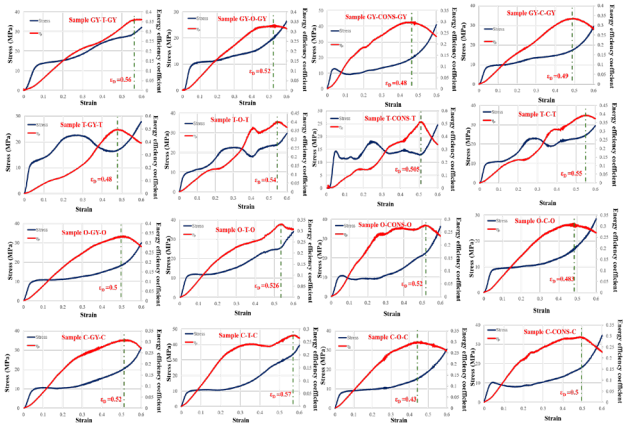

Figure 6 Compression test results of FG samples based on infill pattern.

It was observed that the CONS sample had the highest compression strength among the control samples, and the 70%CONS sample had the highest compression strength among all sample groups (Figure 7). The addition of a section with a 70% infill rate increased the compressive strength of the CONS sample by 54%. The highest yield strength was recorded in the 70%T sample, while the lowest yield strength was measured in the 70%O sample. However, these values are very close to the yield strength values obtained in the T and O control samples, respectively. Regarding the Young's modulus of the samples, the highest value was observed in the T sample as 793.74 ±23 MPa, whereas the lowest value was found in the O sample as 212±12 MPa. Compared to the GY sample, the compressive strength and yield strength increased by 6% and 5%, respectively, in the GY-T-GY samples to which the 2D infill geometry was added. Similarly, the compressive and yield strengths increased by 33% and 6%, respectively, in the GY-CONS-GY sample. In addition, the Young's modulus increased by 22% in the GY-CONS-GY sample compared to the GY sample.

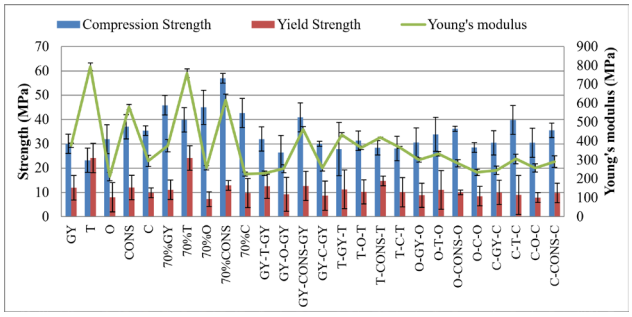

Figure 7 Comparison of compression strength, yield strength and Young's modulus of samples.

Among the control samples, T sample exhibited the highest specific energy absorption capacity. SEA value increased in all samples with the addition of a middle section with a 70% infill rate, and the highest SEA value among them was observed in the 70%CONS sample. The addition of 2D infill patterns such as trihexagonal and concentric to the middle region of the GY sample led to increased SEA values in the GY-T-GY and GY-CONS-GY samples compared to the GY sample.

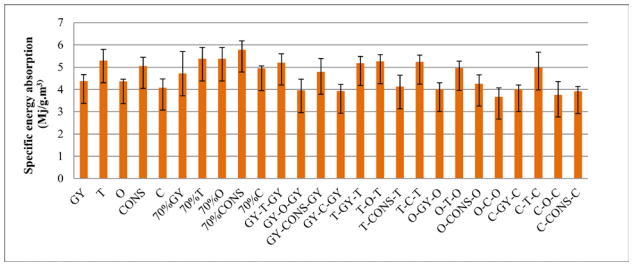

Figure 8 Comparison of the specific energy absorption capacity of test samples.

CONCLUSION

In this study, the effect of functional grading based on infill rate and infill pattern including - 3D patterns (octet, gyroid and cubic) and 2D patterns (trihexagonal and concentric) - on the compressive behavior of porous materials was systematically investigated. 21 functionally graded samples and 5 control samples with uniform porous structures were designed, and all samples were fabricated using fused deposition modeling (FDM). The prominent results of the study are as follows:

-The highest compressive strength among all samples was obtained in the 70%CONS sample with 70% infill rate and was 54% higher than the corresponding control sample.

-The highest yield strength was measured in the 70%T sample and the lowest in the 70%O sample, and these values are very close to the values of the T and O control samples. In terms of Young's modulus, the highest value was determined as 793.74±23 MPa in the T sample, and the lowest value was determined as 212±12 MPa in the O sample.

- All samples FG based on infill rate showed higher compressive strength than the corresponding control samples. In particular, those with 3D patterns were noted for more balanced deformation and late densification zone.

- Integrating a 2D pattern into a 3D structure enhanced compressive strength compared to the control samples.

- The highest specific energy absorption capacity (SEA) was recorded in the T sample in the control group. In all samples functionally graded according to the infill rate, SEA increased compared to the corresponding control samples.

References

1. Campbell I, Bourell D, Gibson I. Additive manufacturing: rapid prototyping comes of age. Rapid Prototyp J. 2012;18(4):255–8.
2. Zaharin HTL, Rani A, Ginta T. Additive manufacturing technology for biomedical components: a review. IOP Conf Ser Mater Sci Eng. 2018;328(1):012007.
3. Gross BC, Erkal JL, Lockwood SY, Chen C, Spence DM. Evaluation of 3D printing and its potential impact on biotechnology and the chemical sciences. Anal Chem. 2014;86(7):3240–53.
4. Durai Murugan P, et al. A current state of metal additive manufacturing methods: a review. Mater Today Proc. 2022;59:1277–83.
5. Zhou L, et al. Additive manufacturing: a comprehensive review. Sensors (Basel). 2024;24(9):2668.
6. Bolat Ç, Çebi A, Ispartalı H, Ergene B, Aslan MT, Göksüzoğlu M. A comparative experimental work on the drop-weight impact responses of thermoplastic polymers produced by additive manufacturing: combined influence of infill rate, test temperature, and filament material. Colloid Polym Sci. 2024;302(12):1967–84.
7. Marşavina L, et al. Effect of the manufacturing parameters on the tensile and fracture properties of FDM 3D-printed PLA specimens. Eng Fract Mech. 2022;274:108766.
8. Pernet B, Nagel JK, Zhang H. Compressive strength assessment of 3D printing infill patterns. Procedia CIRP. 2022;105:682–7.
9. Ivorra-Martinez J, et al. Effect of infill parameters on mechanical properties in additive manufacturing. Procedia Manuf. 2020;95:412–7.
10. Birosz MT, Ledenyák D, Andó M. Effect of FDM infill patterns on mechanical properties. Polym Test. 2022;113:107654.
11. Yadav P, Sahai A, Sharma RS. Strength and surface characteristics of FDM-based 3D printed PLA parts for multiple infill design patterns. J Inst Eng India Ser C. 2021;102(1):197–207.
12. Reichardt A, et al. Advances in additive manufacturing of metal-based functionally graded materials. Mater Des. 2021;66(1):1–29.
13. Tanveer MQ, Haleem A, Suhaib M. Effect of variable infill density on mechanical behaviour of 3D-printed PLA specimen: an experimental investigation. SN Appl Sci. 2019;1(12):1–12.
14. Wen Z, Li M. Compressive properties of functionally graded bionic bamboo lattice structures fabricated by FDM. Materials. 2021;14(16):4410.
15. ASTM International. ASTM D695-15. Standard test method for compressive properties of rigid plastics. West Conshohocken: ASTM International; 2015.
16. Microzey. Microzey PLA Pro Max [Internet]. 2025 Jun 30 [cited 2025 Jun 30]. Available from: https://microzey.com/pla-pro-max
17. ASTM International. ASTM D638-14. Standard test method for tensile properties of plastics. West Conshohocken: ASTM International; 2014.
18. Zhang L, et al. Energy absorption characteristics of metallic triply periodic minimal surface sheet structures under compressive loading. Addit Manuf. 2018;23:505–15.
19. Shinde M, Ramirez-Chavez IE, Potts A, Bhate D. A critical assessment of the onset strain of densification in the evaluation of energy absorption for additively manufactured cellular materials. Manuf Lett. 2024;41:708–19.